

Computational Mesomechanics of Particle-Reinforced Composites

L. Mishnaevsky Jr.^{1,*}, M. Dong^{1,2}, S. Hönl^{1,3} and S. Schmauder¹

¹ *Staatliche Materialprüfungsanstalt (MPA), University of Stuttgart, Pfaffenwaldring 32, 70569 Stuttgart, Germany*

² *Eberspächer GmbH & Co., Eberspächerstraße 24, 73730 Esslingen,*

³ *Robert Bosch GmbH, FV/PL03, P.O. Box 30 02 40, 70442 Stuttgart*

Abstract

Numerical models of deformation, damage and fracture in particle-reinforced composite materials, based on the method of multiphase finite elements (MPFE) and element elimination technique (EET), are presented in this paper. The applicability of these techniques for different materials and different levels of simulation was studied. The simulation of damage and crack growth was conducted for several groups of composites: WC/Co hard metal alloys, Al/Si and Al/SiC composites on macro- and mesolevel. It is shown that the used modern techniques of numerical simulation (MPFE and EET) are very efficient in understanding deformation and damage evolution in heterogeneous brittle/ductile materials with inclusions. © 1999. Elsevier Science B. V. All rights reserved.

1 Introduction

Particle-reinforced composites are widely used industrially. In order to improve their service properties as well as to predict the lifetime of these materials, efficient methods of numerical simulation are necessary. In this paper, modern methods of FE-simulation of deformation, damage and fracture in two phase materials for both 2D and 3D cases are discussed. The possibilities of the methods of multiphase elements and element elimination technique which are used here to study the damage initiation and evolution, and fracture in WC/Co,

Al/Si and Al/SiC composites on meso- and macrolevel, are demonstrated and analysed.

2 Multiphase finite element method (MPFE): main ideas

Consider the main ideas of the multiphase finite element method which has been developed in [1-5]. Commonly, each element of the FE mesh is attributed to one phase; the same material properties are assigned to all integration points of an element and the phase boundaries are supposed to coincide with the edges of finite elements. The idea of the method of multiphase elements

* Corresponding author: Tel.: +49-711-685-3049; fax: +49-711-685-2635. Email address: impgmish@mpa.uni-stuttgart.de

is that the different phase properties are assigned to individual integration points in the element. Therefore, the FE-mesh in this case is independent of the phase arrangement of the material, and one can use relatively simple FE-meshes in order to simulate the deformation in a complex microstructure.

The possibility of using initial meshes of arbitrary simple structures for simulation of the mechanical behaviour of materials with complex microstructure is the main advantage of the method of multiphase elements.

In the case of 3D simulations of the mechanical behaviour of heterogeneous materials with arbitrarily arranged phase boundaries it is almost impossible to construct the FE mesh in such a way that the edges of finite elements correspond to the phase boundaries. Therefore, the possibilities, which the multiphase element method offers are especially important in the 3D case. The 3D version of the MPFE was developed at the Max-Planck-Institut für Metallforschung and at MPA, University of Stuttgart [5,6] and implemented in the commercial FE software LARSTRAN [7].

In the 3D MPFE code, finite elements of low order (with linear or square interpolation functions) are used. The form and distribution of the phases are introduced automatically in the FE model from digitized micrographs of the microstructure. In order to reconstruct the 3D microstructure of material, the following approach is used [5, 6]. Several material layers are metallographically removed equidistantly from the surface of the specimen by careful polishing. Micrographs from each polished surface are made. The thickness of the removed layers must be known for each layer as exactly as possible. Then, the micrographs are digitized with the use of an image analysis software, and the 3D real structure of the material is reconstructed

from the digitized micrographs of the sections.

Each pixel in 2D digitized micrograph is assigned to some volume of material, and therefore determines the correspondence of Gaussian points to the phases in the material. The mechanical properties of the phases are automatically assigned to the integration points.

3 Element elimination technique for simulation of damage in two-phase materials

3.1. Element elimination technique

The element elimination technique (EET), developed in [1, 3], is based on the quasi-removal of finite elements, which satisfy some failure condition (which is to be defined for each material to be considered). In such a way the formation, growth and coalescence of voids or microcracks, and the crack growth are simulated. As criteria of local failure, both global (external loads or displacement) and local (i.e. defined for a given element; for instance, plastic strain, von Mises stress, hydrostatic stress, etc) values as well as any combination of these values can be used. Besides, EET can be used both for multiphase and single phase materials (in so doing, the criteria of element elimination should be chosen separately for each phase of the multiphase material).

The local values are calculated in the following succession: first, local displacements are calculated, then, strains, thereafter, stresses, and finally, forces [3]. As a result of this chain, the reaction forces are calculated for each node of the FE mesh. After applying the external displacements non-equilibrium state of all the structure is established. Since the stiffness matrix depends on the displacements in the nodes,

the displacements are corrected in several iterative steps until force equilibrium is established. When the structure is balanced, one decides for each finite element whether it has to be eliminated or not [3].

To eliminate an element, all components of the stress tensors in this element are set to zero. As a result, all forces in this element become zero as well, and therefore, this element stops to transmit load to neighbouring non-eliminated elements. So, the element elimination does not mean that an eliminated element is really removed from the FE mesh, but stops to interact with neighbouring elements. In solving the problem the tangential stiffness matrix should be corrected after the element elimination. This is done by setting Young's modulus of eliminated elements to be equal to zero. J. Wulf noted that Drucker's stability condition is not obeyed in the element elimination, what can lead to some numerical problems during the simulation [3]. In order to avoid numerical problems related to strong local loss of equilibrium, the stresses are set to be equal to zero in several steps (called "relaxation steps"). The Young's moduli in eliminated elements are set to be equal to zero in the last relaxation step [3].

3.2. Conditions of element elimination

The above described procedure allows to simulate damage initiation as well as crack growth in different materials. The interrelation between the element elimination approach and models of crack growth caused by the formation of voids in front of the crack has been given in [8].

A criterion of element elimination which is appropriate for each material should be chosen by comparison of numerical and experimental results as well as by experimental studying micromechanisms of damage initiation. For instance, Wulf used the condition of critical plastic strain as crite-

riion for element elimination [3]. Lippmann et al. [9] and Hönle et al. [10] have used a two-criteria model of element elimination for the simulation of AlSi cast alloys: elements which were assigned to hard (Si) particles, were eliminated on the basis of a normal stress criterion, and the critical value for failure of the ductile matrix phase was simulated using a damage-parameter, which is based on the work of Rice&Tracey [11] and Hancock&Mackenzie [12, see also 13]. The damage parameter can be written as [14, see also 3]

$$D = \int_0^{\varepsilon_{pl,c}} e^{3/2\eta} d\tilde{\varepsilon}_{pl}$$

with failure initiation at a critical damage parameter value of D_c . Here ε_{pl} – effective plastic strain, $\varepsilon_{pl,c}$ – critical plastic strain, η – stress triaxiality, $\eta = \sigma_H/\sigma_V$, σ_H - hydrostatic stress, and σ_V – von Mises equivalent stress. The damage parameter fulfils all demands on locality, triaxiality of the stress-strain field, as well as taking into account the complete failure history.

The damage parameter (1) can be generalised in order to take into account the so-called "failure curves" of materials in the following way. Failure curves (see Figure 1) present a relation between equivalent plastic strain and stress triaxiality at the crack initiation point inside the specimen, obtained on the basis of combined experimental and numerical investigations on tensile specimen [15, see also 10]. The failure curve separates the equivalent plastic strain - stress triaxiality space into two parts. Below the curve the material is save, no failure will occur. Points on the curve indicate failure initiation for a given stress-strain field. If one expresses the failure curves as shown in Figure 1 as

$$\varepsilon_{pl,c} = A \cdot e^{-B\eta_c}$$

(2)

where A and B are two material dependent parameters, and assuming that usually $\varepsilon_{pl} \leq \varepsilon_{pl,c}$ and $\eta \leq \eta_c$ holds during loading, one can derive the modified damage parameter [10]:

$$D = \frac{1}{A} \int_0^{\varepsilon_{pl,c}} e^{B\eta} d\tilde{\varepsilon}_{pl} \quad (3)$$

with the point of failure initiation at a critical damage parameter value of $D_c=1$.

3.2. Determination of the condition of element elimination: an example

To demonstrate how the condition of element elimination can be determined from experimental data, let us consider a simple macroscopical simulation of crack growth in Al/SiC (20 vol. %) composites under 3-point-bending. A FE mesh similar to the mesh given in [3] was taken in the simulation. However, a criterion of element elimination different from that used in [3] was applied: instead of the critical plastic strain, the Rice&Tracey damage parameter was chosen as criterion for element elimination. The calculations were carried out for a material with averaged elastic properties of the specimen ($E=99.4$ GPa and $\nu=0.323$). The difference between the critical plastic strain and Rice&Tracey's damage criterion for element elimination is determined by the fact that the Rice&Tracey damage criterion is very sensitive to the degree of triaxiality in the deforming material, while this is not the case for the critical plastic strain criterion. The finite elements which are located on the loading surface were assumed to be elastic and were not subject to damage in order to simplify the simulation of the specimen/holder contact conditions. Basing on the available data about the critical values of damage [3, 7, 9] we used three different values of critical damage parameters: $D_c = 0.1, 0.15$ and 0.2 . As a result, the force-

displacement curves for the specimen were obtained. The curves for the different values of the critical damage parameter are shown in Figure 2. Although the peak points of the force-displacement curve were determined correctly and correspond to the experimental data the appearance of the descending branch of the curve differs significantly from the experimentally observed results [3]. The values of the calculated peak load for the different critical damage parameters as well as the experimentally obtained peak load are given in Table 1. It is found that the critical damage parameter $D_c=0.2$ results in simulating the correct peak load. Therefore, our results confirm the data from [3, 10], that the critical value of Rice&Tracey's damage parameter for Al/ 20 vol. % SiC should be taken as $D_c=0.2$. The described procedure shows how the criterion of element elimination can be determined by comparing the experimental and numerical force-displacement curve.

4 Mesomechanical modelling of damage and failure in real structures

In this section, the model of damage initiation and growth, and fracture in a material with real structure is presented. In this model, both the multiphase element method and the element elimination technique are used. The simulation is carried out for WC-Co hard metals, which present particle-reinforced composites with coarse microstructure; these materials are characterised by a typically high content of hard inclusions and their relatively large size as compared with the thickness of areas of Co binder. A model microstructure of WC/Co material was taken and used in the simulations. The WC/Co specimen possesses a cobalt volume fraction of 16% and an average carbide size of $1.5 \mu\text{m}$.

The microstructure is meshed using multi-phase elements (MPFE) and is embedded in an environment with the elastic material behaviour of the composite and a pre-crack just in front of the real structure (Figure 3).

The material properties of the carbide are elastic and the elastic-plastic behaviour of the cobalt is represented by a modified Voce-type flow law with an additional Hall-Petch term [10], according to

$$\sigma = \sigma_y + (\sigma_s - \sigma_y) \cdot \left[1 - \exp\left(-\frac{\epsilon}{\epsilon^*}\right) \right] + k_y L^{-1/2} \quad (4)$$

where $\sigma_y=270$ MPa – yielding stress of cobalt, $\sigma_s=970$ MPa, $\epsilon^*=0.06$, $k_y=7$ Nmm^{3/2} (material constants) and an average binder layer thickness of $L=0.5$ μm were taken from [16].

Critical plastic strains and stress triaxialities, which were derived using crystal plasticity theory [17] at a critical void volume fraction of 15% [18] are shown in Figure 1. These results lead to the modified damage parameter,

$$D = \frac{1}{1.04} \int_0^{\epsilon_{pl,c}} e^{1.12\eta} d\tilde{\epsilon}_{pl} \quad (5)$$

In the following, results of a crack propagation simulation based on equation (5) are described.

As a first attempt, a hard metal with a high cobalt content and no contact between carbide particles was modelled and investigated under external tensile loading (see Figure 4a). This study focused on the failure behaviour of the ductile cobalt phase. Brittle fracture in the carbide phase was thus suppressed. At considered level (mesolevel) the structure of material was

practically random, and therefore, no special consideration of the texture dependence was required in this case. The results achieved on the level of crystal plasticity were calculated for a wide range of microscopic arrangements and crystallographic slip system arrangements, and thus describe an averaged behaviour of the material based on crystal plasticity theory.

Figures 4b, 4c, 4d and 4e show crack initiation and crack propagation in this structure. The crack enters the real structure by initiating a void (Figure 4b), which starts to grow under increasing load. Further increase of the applied load leads to void initiation in front of the crack tip (Figures 4c and 4d) and coalescence with the main crack. Crack propagation is found to be a consequence of nucleation, growth and coalescence of the voids. This numerical study is in agreement with experimental findings on WC/Co hard metals [19]. The force-displacement curve for this crack propagation depicts the experimental macroscopic failure behaviour of WC/Co hard metals as a quasi brittle failure. The applied load increases nearly linearly, while it drops immediately when the critical load is reached.

Thus, local damage behaviour of the ductile cobalt phase is introduced in microscopic crack propagation simulations by making use of failure curves.

5 Meso-macromechanical modelling of damage and failure of two-phase composites

5.1 Microdamage in Al/Si cast alloys: unit cell simulation

In Al/Si cast alloy specimens the damage process is determined by the strength of Si-particles and the Al-matrix as well as the shape, size, arrangement and volume fraction of the Si-particles. The Si-particles behave elastic and the Al-matrix elasto-plastic. It is known that only large Si-particles fracture during external loading [8, 9]. Large particles are present at a low volume fraction of about 1~5% in the alloy, while the overall volume fraction of Si amounts to 12%.

In the mesomechanical model a unit cell containing a silicon particle and the aluminum matrix is embedded in an equivalent homogeneous material with the same mechanical behaviour as that of the embedded cell (Figure 5). Under the tensile displacement loading of the upper external boundary of the embedding composite in the cell shown in Figure 5, the overall response of the inner embedded cell is obtained by averaging the stresses and strains in the embedded cell [20]

Microdamage of the two-phase material in the embedded cell [20] is simulated by a hybrid local approach for brittle cracking of silicon particles and for ductile failure of the aluminum matrix (Figures 5 and 6). The normal stress criterion ($\sigma_{\max}^n=320$ MPa obtained from comparison of simulation and experiment in [21]) and node release technique are applied to simulate Si-particle cracking whereas the damage parameter D and the element elimination technique (EET) are applied for simulating ductile void growth in the Al-matrix. The damage parameter involves the loading state as well as the loading history and its critical value can be derived from the corresponding experiment and simulation (in this case, $D_c=0.7$ [22]).

At a total strain of $\epsilon_{\text{tot}}=0.43\%$ the Si-particle is cracking orthogonally with respect to the tensile loading direction according to the normal stress criterion and

then matrix damage occurs subsequently under increasing loading. The matrix damage propagates in the same direction as the Si-particle crack. Local stress-strain relations of the Al/12%Si cast alloy concerning both particle failure and matrix damage are thus obtained for different volume fractions of locally damaged material (Figure 5), which are further taken into account in the macromechanical model.

The local damage-parameter distribution in the embedded cell for three different loading steps (Figure 6) shows the development of damage parameter concentration, which results in void growth and crack propagation in the matrix. The released energy is an important magnitude for comparison with the nondestructive evaluation of damage by acoustic emission.

From local energy considerations the energy release rate by further damage propagation can be calculated as a function of microcrack length (Figure 7). After fracture of the silicon particle the energy release rate of the matrix damage increases with sub-critical microcrack growth until rupture of the material.

5.2 Macromechanical model of failure in AlSi cast alloys

On the basis of the above described mesomechanical model, macromechanical models of tensile or compressive specimens are set up to investigate crack growth. The mechanical behaviour of the Al/12%Si cast alloy with damage evolution was assigned to each finite element taking into account damage initiation and propagation calculated from the mesomechanical models presented above. In this way the macroscopical development of microdamages until rupture of the specimen can be

simulated. As an example, an initial Si-failure is introduced at a corner of a homogeneous specimen. The propagation of Si-failure is calculated according to the critical normal stress obtained from micro-modelling.

The simulations demonstrate two stages of damage evolution: At first the Si-particles fail along shear bands which nucleate from the initial failure side in the specimen at the macroscopic plastic flow stage, as shown in the stress distribution in Figure 8. After Si-failure the specimen can still carry increased loading and stretching. Under further loading the damage parameter concentration increases in the cross section orthogonally to the loading direction and the crack starts to propagate perpendicular to the loading direction until failure of the specimen in agreement with observations of fracture in such materials [20] (Figure 8).

6 3D FE simulation of deformation in real structures

In this section, the results obtained by Mishnaevsky Jr et al. [6] in the framework of the COST-Project “Microstructural investigation of failure mechanisms in AlSi-cast alloys by 3D FE-modelling” are reported and compared with above described 2D models of mechanical behaviour of composites. To simulate the deformation of specimens from AlSi cast alloys with different microstructures, 3D MPFE has been applied.

The small volume in which the real structure was reconstructed is located in the notch region of loaded compact tension (CT) specimen. The scheme of loading CT specimen is shown in Figure 9. For a small volume (100 μm x 100 μm) in the notch ground region the microstructure of material was reconstructed with the use of digitized micrographs of polished sections as described above. The properties of components (Al matrix and Si particles) have

been assigned to finite elements in correspondence with distribution of “black” and “white” areas on digitized micrographs. The rest of the specimen was assigned the averaged properties of AlSi cast alloy. In the area of real microstructure there were 4 000 finite elements, in the full specimen 16 000 FE. The simulation was carried out for two alloys: one with lamellar and one with globular microstructures. The load was increased in 5 loading steps, each was 100 N. The mechanical properties and stress-strain curve of Al matrix and Si particles have been determined experimentally as described in [6].

Some results of the simulation are shown in Figure 10: the von Mises stress distribution in the region with real structure for both types of the alloy microstructure. The von Mises stress distribution is presented in order to study the effect of Si-particles on the stress field in the material. From Figure 10 one can see that the Si-particles cause high local stress concentrations, especially on the notch surface. One may suppose that the high local stress concentrations lead to damage initiation in the vicinity of Si-particles. The experimental investigations of damage evolution in AlSi cast alloys [6, 21, 23] confirm this assumption: microcracks have been formed in the vicinity of Si-particles, often near the notch surface, and then grow and form large cracks.

The developed approach permits 3D finite element simulations of deformation and local effects in heterogeneous materials, using the reconstructed real structures and the method of multiphase elements. However, the accuracy of 3D simulation depends strongly on the degree of fineness of the FE mesh and on the amount and quality of layers (sections) from which the 3D real structure is reconstructed. For both factors, there are unavoidable limitations (computational and experimental, respectively), which limit the possibility of this model.

7 Conclusions

In this paper, the results of application of advanced numerical methods (MPFE and EET) for the simulation of the mechanical behaviour and failure of particle-reinforced composites were presented.

Several aspects of FE simulation of particle-reinforced composites were considered:

- method of determination of conditions of local failure;
- modelling of deformation and fracture in coarse particle-reinforced composites (WC-Co hard metals, in this case);
- multilevel modelling of deformation and fracture of composites with fine particles; transition from a mesomechanical model of behaviour of composites with relatively fine particles (AlSi) to the macroscopical model of material;
- possibility of generalisation of 2D methods of FE simulation of materials with real structures to the 3D case.

The methods are applied to model the mechanical behaviour of different types of materials: quasi-homogeneous (macro-models of AlSi and AlSiC), coarse particle-reinforced composites (WC-Co hard metals) and fine particle-reinforced composites with different types of microstructures (lamellar, globular) (AlSi).

A mesomechanical model of damage and fracture of hard metals made it possible to determine the mechanisms of fracture. It is shown numerically that crack propagation can be simulated as a result of nucleation, growth and coalescence of voids. The force-displacement curve for this crack propagation depicts the experimental macroscopic failure behaviour of WC/Co hard metals as a quasi-brittle failure: the applied load increases nearly linearly, while it drops immediately when a critical load is reached. The local damage behaviour of

ductile cobalt phase in hard metals was taken into account in the simulations by using the failure curves.

The possibility of generalisation of the FE model of the mechanical behaviour of material for the 3D case has been explored. Although there are some essential limitations in the used experimental and numerical techniques, related with the difficulties of obtaining many micrographs of sections of a material volume with strictly equal distances between them, and the limited amount of elements in the mesh, which must be however very fine, this first trial of 3D simulation of deformation of real structures has demonstrated possibilities of this approach.

Although the purely one-scale level models are appropriate for solving some partial problems (like the quasi-homogeneous model for the determination of the condition of element elimination in the material with low filler content, and the mesomodel for the simulation of coarse composites like hard metals), the multilevel approach seems to be more promising, and can allow to describe the behaviour of material taking into account real physical mechanisms of material behaviour.

Thus, the meso-macromechanical model allow to simulate the damage evolution and failure in an AlSi alloy. The mechanism of failure of the alloy has been clarified. It has been shown numerically, that the failure of a large Si-particle causes subsequent damage of the Al-matrix on the micro-level. It is found that Si-particle cracking takes place at much higher loading levels in compression than in tension and no further Al-matrix damage occurs. After cracking of the Si-particle, the material can be further loaded. Sub-critical crack growth induces plastic deformation in the matrix. Si-particles fail in macroscopic shear bands which are initiated at crack tips before ductile rupture of the specimen

in the main crack plane perpendicular to the loading direction.

8 Acknowledgements

The authors gratefully acknowledge the financial support by the Deutsche Forschungsgemeinschaft (DFG) via the Sonderforschungsbereich 381 "Charakterisierung des Schädigungsverlaufes in Faserverbundwerkstoffen mittels zerstörungsfreier Prüfung" (Characterization of damage evolution in fiber reinforced composites using nondestructive testing methods) and the European Commission for financial support via the Brite-Euram Project 8109 "Design of new tool materials with a structural gradient for milling application" and ECSC-Project 8834 "Influence of micromechanical mechanisms on strength and damage of tool steels under static and cyclic loading".

9 References

- 1 Th. Steinkopff, M. Sautter, und J. Wulf, Mehrphasige Finite Elemente in der Verformungs- und Versagenanalyse grob mehrphasiger Werkstoffe. Arch. Appl. Mech. 65, 1995, pp. 495-506
- 2 Th. Steinkopff and M. Sautter, Simulating the Elasto-plastic Behavior of Multiphase Materials by Advanced Finite Element Techniques. Comp. Mat. Sci. 4, 1995, pp. 10-22
- 3 J. Wulf, Neue Finite-Elemente-Methode zur Simulation des Duktilbruchs in Al/SiC. MPI für Metallforschung, Stuttgart, 1995, 205 pp.
- 4 M. Sautter, Modellierung des Verformungsverhaltens mehrphasiger Werkstoffe mit der Methode der Finiten Elemente, Fortschr.-Ber.VDI, Reihe 5, Düsseldorf, 1995, 210 pp.
- 5 N. Lippmann, Th. Steinkopff, S. Schmauder and P. Gumbsch, 3D-Finite-Element-Modelling of Microstructures with the Method of Multiphase Elements", Comput. Mat. Sci., Vol. 9, 1997, pp. 28-35
- 6 L. Mishnaevsky Jr, N. Lippmann, P. Gumbsch, S. Schmauder, H.-J. Spranger and E. Arzt, Mikrostrukturelle Untersuchung der Versagensmechanismen in AlSi-Gußlegierungen mit 3D-FE-Analysen, BMBF Project report, MPA Stuttgart, 1998, 102 pp.
- 7 LARSTRAN, LASSO Ingenieurgesellschaft, Leinfelden-Echterdingen, Germany
- 8 L. Mishnaevsky Jr, O. Minchev and S. Schmauder, FE-Simulation of Crack Growth Using Damage Parameter and the Cohesive Zone Concept, with In: "ECF 12 - Fracture from Defects", Proc. 12th European Conference on Fracture (Sheffield, 1998). Eds. M.W. Brown, E.R. de los Rios and K. J. Miller. EMAS, Vol. 2, pp. 1053-1059
- 9 N. Lippmann, S. Schmauder and P. Gumbsch, Numerical and Experimental Study of the Failure Mechanisms in AlSi-Cast Alloys, in "Localized Damage IV", eds. by H. Nisitani et al., Computational Mechanics Publications, Southampton, UK, 1996, pp. 333-340
- 10 S. Hönle, M. Dong, L. Mishnaevsky Jr and S. Schmauder, FE-Simulation of Damage Evolution and Crack Growth in Two-Phase Materials on Macro- and Microlevel on the Basis of Element Elimination Technique and Multiphase Finite Elements. Proceedings 2nd Europ. Conf. Mechanics of Materials, Eds. A. Bertram et al., Magdeburg, 1998, pp. 189-196
- 11 J.R. Rice and D.M. Tracey, On the Ductile Enlargement of Voids in Triaxial Stress Fields, Int. J. Mech. Phys. Solids 17, 1969, pp. 201-217
- 12 J.W. Hancock and A.C. Mackenzie, On the Mechanisms of Ductile Failure in High-Strength Steels subjected to Multi-Axial Stress-States, J. Mech. Phys. Sol. 24, 1976, pp. 147-167
- 13 F.D. Fischer, O. Kolednik, G.X. Shan and F.G.Rammerstorfer, A Note on Calibration of Ductile Failure Damage Indicators. Int. J. Fracture. 73, 1995, pp. 345-357
- 14 S.R. Gunawardena, S. Jansson and F.A.Leckie, Modeling of Anisotropic Behavior of Weakly Bonded Fiber Reinforced MMC's, Acta met. mater. 41, 1993, pp. 3147-3156
- 15 J. Arndt, F. Grimpe and W.Dahl, Influence of Strain History on Ductile Failure of Steel, In: Mechanisms and Mechanics of Damage and Failure of Engin. Materi-

- als and Structure (Proc. Int. Conf. ECF-11), Eds. J. Petit et al, Vol. 2, EMAS, London, 1996, pp. 799-804
- 16 M.-H.Poech, H. F. Fischmeister, D. Kaute and R. Spiegler, FE Modelling of the Deformation Behaviour of WC/Co Alloys. , Comput. Mat. Sci., Vol. 1, 1993, pp. 213-
- 17 P.J. Connolly, P.E. McHugh, Fracture Modelling in Metal Ceramic Composites using the Gurson Model and Crystal Plasticity Theory, Presentation at 7th International Workshop on Computational Modelling of Materials, Vienna, 1997 (to be published in Comp. Mater. Sci.)
- 18 W. Brocks, S. Hao and D. Steglich, Micromechanical Modelling of the Damage and Toughness Behaviour of Nodular Cast Iron, J. de Physique IV (1996) C6, 43-52.
- 19 L. Sigl. Das Zähigkeitsverhalten von WC-Co-Legierungen. VDI Fortschritt-Berichte, 5, No. 104, VDI Verlag, Düsseldorf, 1986
- 20 M. Dong, S. Schmauder. Modeling of Metal Matrix Composites by a Self-Consistent Embedded Cell Model, Acta mater. 44, 1996, pp. 2465-2478.
- 21 N. Lippmann, S. Schmauder and P. Gumbsch, Numerical and Experimental Study of Early Stages of the Failure of AlSi-Cast Alloys. J. de Physique IV (1996) C6, 123-131.
- 22 S. Schmauder, M. Dong, Micro-, Meso- and Macromechanical Modeling of Damage in an Al/Si Cast Alloy, Proc. 6th Int. Symposium on Plasticity and its Current Applications, Ed.: A. S. Khan, Neat Press, Fulton Maryland, 1997, pp. 275-276.
- 23 L. Mishnaevsky Jr, N. Lippmann, S. Schmauder and P. Gumbsch, In-situ Observation of Damage Evolution and Fracture in AlSi7Mg0.3 Cast Alloys Eng. Fract. Mech., Vol. 63, Nr. 4, 1999, pp. 395-411

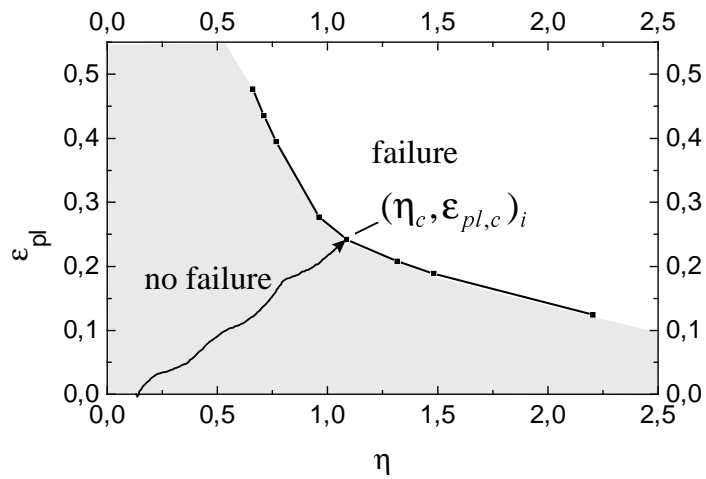


Figure 1: Scheme of a failure curve.

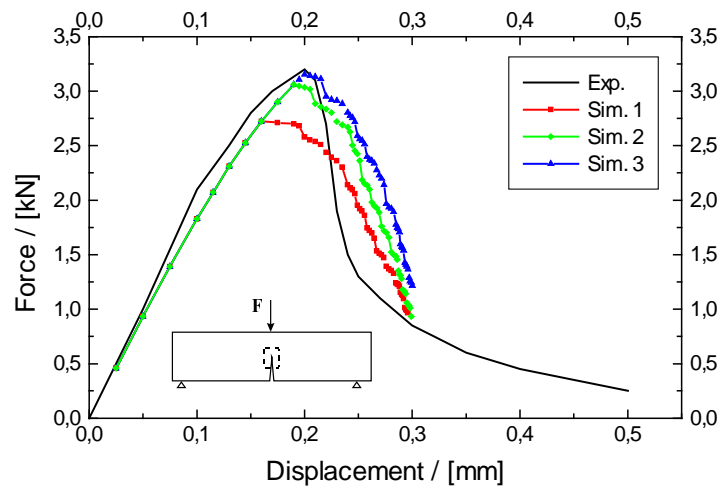


Figure 2: Force-displacement curves for 3-point-bending.
 Sim. 1 ($D_c=0.2$), Sim. 2 ($D_c=0.15$), Sim.3 ($D_c=0.10$).

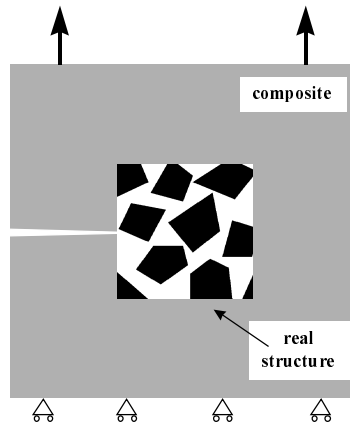


Figure 3: Micromechanical model for failure simulation in realistic structures.

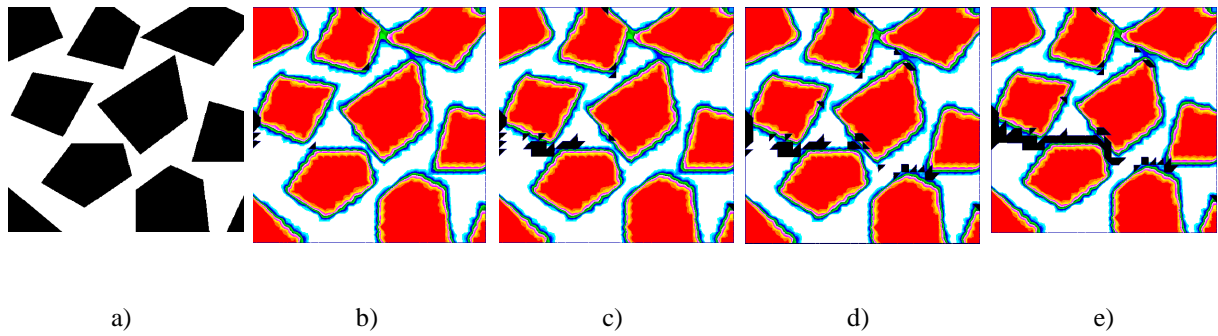


Figure 4: a) Idealised real structure (WC black, Co white), b) - e) void nucleation, growth and coalescence.

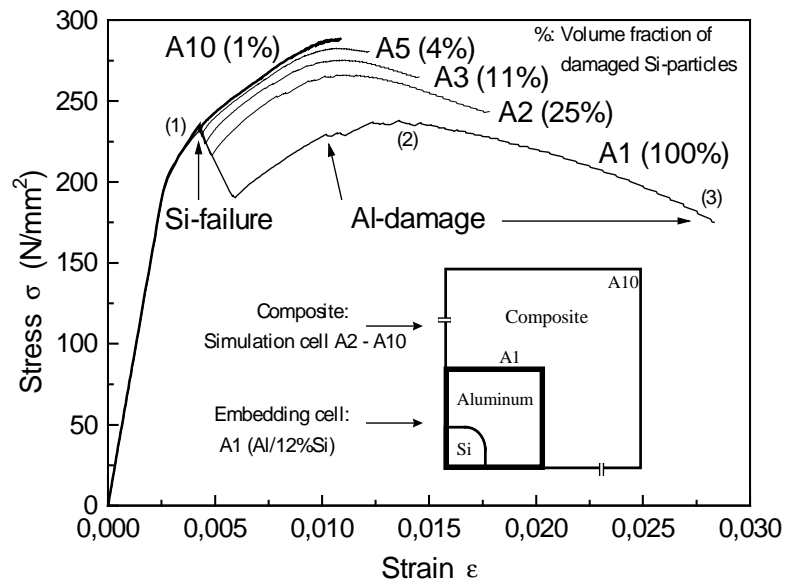


Figure 5: Local stress-strain relations of the Al/12%Si cast alloy concerning both particle cracking and matrix failure for different volume fractions of locally damaged material.

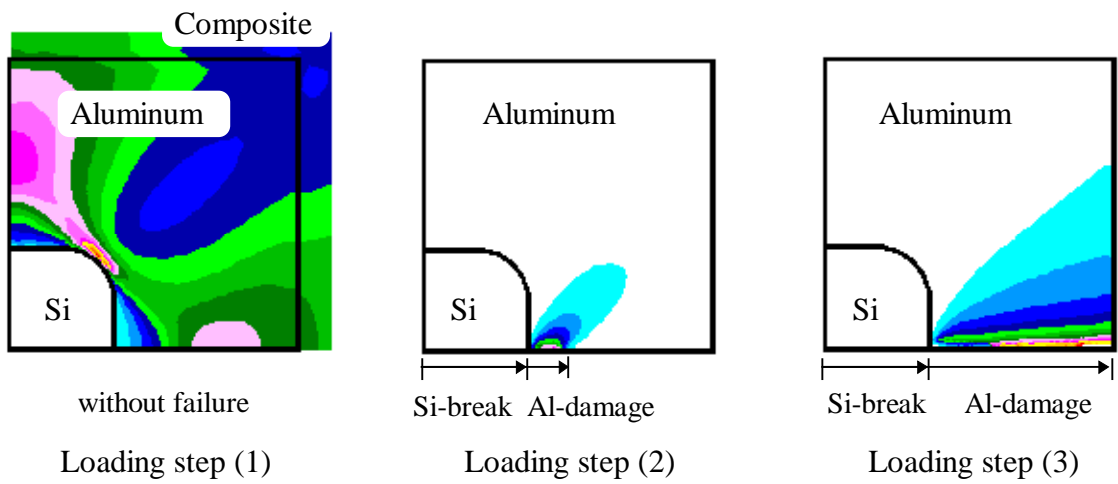


Figure 6: Local damage-parameter distribution in the embedded cell for three different loading steps according to Figure 5. White areas: $D=0$, very bright areas: $D=0.6...0.7$, dark areas: $D=0.4..0.5$, medium dark till bright areas: $D=0.1...0.3$.

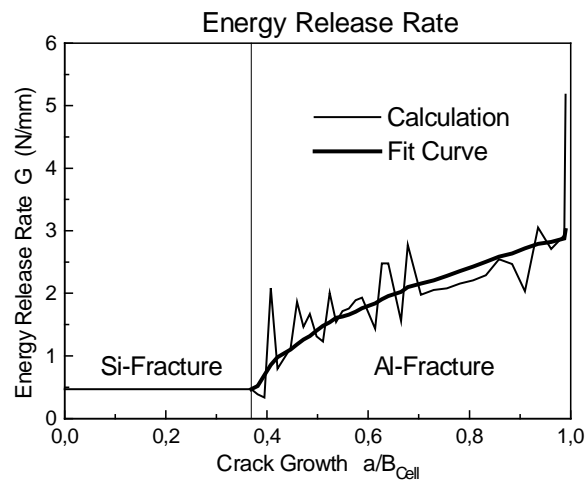


Figure 7: Energy release rate of matrix damage after silicon particle cracking.

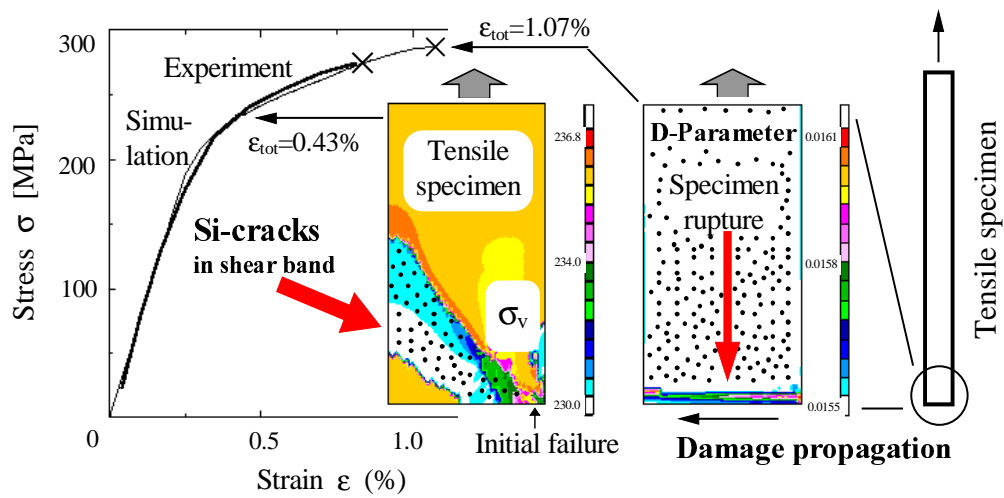


Figure 8: Macroscopical development of microdamages at different loading stages (Areas of cracked Si-particles are represented by black dots).

Critical damage parameter, D_c	0.1	0.15	0.2	Experiment [3]
Peak loads, kN	2.76	2.95	3.1	3.1
Displacement, mm	0.22	0.24	0.26	0.2

Table 1: Peak loads on the force-displacement curves at different critical values of Rice&Tracey's damage parameter.